Tetrahymena Meiotic Nuclear Reorganization Is Induced by a Checkpoint Kinase–dependent Response to DNA Damage

Josef Loidl* and Kazufumi Mochizuki†

*Department of Chromosome Biology and Max F. Perutz Laboratories, Center for Molecular Biology, University of Vienna, A-1030 Vienna, Austria; and †Institute of Molecular Biotechnology of the Austrian Academy of Sciences (IMBA), A-1030 Vienna, Austria

In the ciliate *Tetrahymena*, meiotic micronuclei (MICs) undergo extreme elongation, and meiotic pairing and recombination take place within these elongated nuclei (the "crescents"). We have previously shown that elongation does not occur in the absence of Spo11p-induced DNA double-strand breaks (DSBs). Here we show that elongation is restored in *spo11Δ* mutants by various DNA-damaging agents including ones that may not cause DSBs to a notable extent. MIC elongation following Spo11p-induced DSBs or artificially induced DNA lesions is probably a DNA-damage response mediated by a phosphokinase signal transduction pathway, since it is suppressed by the ATM/ATR kinase inhibitors caffeine and wortmannin and by knocking out *Tetrahymena*'s *ATR* orthologue. MIC elongation occurs concomitantly with the movement of centromeres away from the telomeric pole of the MIC. This DNA damage–dependent reorganization of the MIC helps to arrange homologous chromosomes alongside each other but is not sufficient for exact pairing. Thus, Spo11p contributes to bivalent formation in two ways: by creating a favorable spatial disposition of homologues and by stabilizing pairing by crossovers. The polarized chromosome orientation inside the crescent resembles the conserved meiotic bouquet, and crescent and bouquet also share the putative function of aiding meiotic pairing. However, they are regulated differently because in *Tetrahymena*, DSBs are required for entering rather than exiting this stage.

INTRODUCTION

When eggs or sperm are produced, they must be furnished with a single set of chromosomes. Therefore, diploid germ progenitor cells undergo a reductional division, meiosis. During meiosis, homologous chromosomes of paternal and maternal origin exchange parts and segregate to different daughter nuclei. Errors in this process lead to congenital defects in the progeny, stillbirths, or miscarriages in humans.

For homologous chromosomes to recombine and segregate, they must first pair. To this end, chromosomes identify each other, align, and finally become closely linked by the synaptonemal complex (SC). These events are accompanied by the formation of the bouquet, which is a widely conserved arrangement of chromosomes. It is characterized by the congression of telomeres at the inner surface of the nuclear membrane (Zickler and Kleckner, 1998; Scherthan, 2001). It is not yet clear whether and how the bouquet supports the mutual recognition and/or synapsis of homologues. Simultaneous pairing and initiation of synapsis of chromosomes in the bouquet was demonstrated by Scher-

than *et al.* (1996) and Bass *et al.* (2000). In other cases, it appears that the assembly of telomeres at the nuclear periphery facilitates the initiation of synapsis in distal chromosome regions (Moens *et al.*, 1989; Alsheimer *et al.*, 1999). Chromosome movement accompanying bouquet formation and resolution may help to resolve interlocking, i.e., the capturing of other chromosomes between two synapsing homologues (Koszul *et al.*, 2008 and references therein).

During meiosis, programmed DNA double-strand breaks (DSBs) are formed by Spo11p, which establishes covalent bonds with flanking DNA segments. These DSBs are processed in a particular way that involves the removal of Spo11p and the formation of 3' DNA overhangs that can invade homologous duplex DNA and thereby initiate strand exchange and meiotic recombination (Keeney, 2007). The resulting chiasmata are crucial in defining the partners to be segregated. Meiotic DSBs (like other DNA alterations) trigger phosphokinase signal transduction pathways that, on the one hand, activate processes leading to the repair of DSBs by homologous recombination and suppress undesired alternative repair and on the other hand, arrest meiotic cell cycle progression until repair is achieved (Hunter, 2008; Longhese *et al.*, 2008).

Tetrahymena thermophila is a ciliated protist with an unusual meiosis. Ciliates are unicellular organisms with two nuclei, a large polyploid macronucleus (MAC) and a diploid micronucleus (MIC) that represents the germ line and undergoes meioses. The MAC is decomposed during meiosis and regenerated from the MIC during the development of sexual progeny (Collins and Gorovsky, 2005). When two cells of different mating types meet and conjugate, meiosis is

induced in both cells. Meiosis in *Tetrahymena* is remarkable because of the likely absence of an SC (Wolfe *et al.,* 1976; Loidl and Scherthan, 2004) and the extreme elongation of the MIC to ~50 times its normal diameter during meiotic prophase (Ray, 1956). Telomeres and centromeres occupy positions at opposite ends of this elongated MIC (also known as the crescent; Cui and Gorovsky, 2006; Mochizuki *et al.,* 2008). The resemblance of this polarized chromosomal arrangement inside the crescent nucleus to the bouquet suggests that it serves a conserved role in meiosis. In *Tetrahymena,* chromosome pairing and recombination take place in the elongated MICs, and it was suggested that the alignment of corresponding chromosome regions may be enforced by the shape of the nucleus together with the bouquet-like arrangement of chromosomes (Loidl and Scherthan, 2004; Mochizuki *et al.,* 2008).

The coordination of meiotic events at the molecular (DSB formation and strand exchange) and cellular (chromosome pairing and chiasma formation) levels is poorly understood. We have shown previously that the activity of Spo11p (most likely due to its inducing DSBs) is required for full MIC elongation (Mochizuki *et al.,* 2008). Here, we investigate in more detail the factors that regulate MIC elongation, and we study the consequences of suppressed MIC elongation in wild-type cells on the bouquet-like arrangement and pairing of chromosomes. Our results provide evidence for the central role of DNA lesions (in the wild-type situation: DSBs) in eliciting a signal response that coordinates chromosome pairing with molecular recombination to ensure that crossing over takes place between homologous rather than sister or homeologous DNA molecules.

MATERIALS AND METHODS

Strains and Growth Conditions

Tetrahymena thermophila (previously known as *T. pyriformis*) cells were grown in liquid culture at 30°C according to standard methods (see Orias *et al.,* 2000). Strains B2086 and CU428 were used as the wild-type control. *spo11* somatic knockout strains (*spo11Δ*) were described previously (Mochizuki *et al.,* 2008). Cells were made competent for conjugation by starvation in 10 mM Tris-HCl (pH 7.4) for 16–24 h. Conjugation and meiosis were induced by mixing starved cultures of two wild-type or mutant strains at equal cell densities (~2 × 10^5 cells/ml). For cytological inspection, aliquots of conjugating cultures were drawn at the indicated time points.

ATR1 Deletion by Macronuclear Gene Replacement

The disruption construct for ORF TTHERM_01008650 (*ATR1*) was made as described (Mochizuki *et al.,* 2008). In short, a genomic region flanking the 5′ end of the *ATR1* gene was amplified by PCR with primers ATR1KO5FW (5′-TCC TCT TTA GGT GGT AGT CG-3′) and ATR1KO5RV (5′-GTC TAT CGA ATT CCT GCA GCC CTG TGG ATT AAA GAC TCA G-3′) in which the underlined sequence is complementary to the 5′-arm of the *neo4* cassette. A genomic region 3′ of the *ATR1* gene was also amplified by PCR with primers ATR1KO3FW (5′-CTG GAA AAA TGC AGC CCT GAA GAA GGC ATA GAC AGT C-3′, in which the underlined sequence is complementary to the 3′-arm of the *neo4* cassette, and ATR1KO3RV (5′-GGA GAG AAT GAG GCA GAT CG-3′). Three pieces of DNA, the 5′-flanking sequence, the SmaI-digested *neo4* cassette, and the 3′-flanking sequence were then connected and amplified by overlapping PCR using ATR1KO5FW and ATR1KO3RV. The PCR product was used for biolistic transformation into the macronuclear *ATR1* loci of B2086 and CU428 cells. The transformants were exposed to increasing concentrations of paromomycin to gradually select for replacement by the deletion construct due to phenotypic assortment (Cassidy-Hanley *et al.,* 1997).

Irradiation of spo11Δ Cells

Irradiation of conjugating cells was performed 2 h after cell mixing. For UV exposure, 5 ml of cell suspension were spread out to a thin layer in an 8.5-cm polystyrene Petri dish. A Stratalinker UV cross-linker was used for the acute exposure of cells to 254 nm UV (UV-C) at a dosage of 20 Joule/m² (=2.000 μJ/cm²). Treatment with ionizing radiation was performed by exposure to 5000 rads of γ-radiation from a ⁶⁰Co source. Irradiated cells were then cultured for another 1.5 h and fixed by one of the methods below.

Chemical Treatments

Conjugating cells were treated with one of the following substances: cisplatin, methyl methane sulfonate (MMS), benomyl (methyl [1-[(butylamino)carbonyl]-1H-benzimidazol-2-yl]carbamate), nocodazole, caffeine, or wortmannin. Benomyl was a gift from DuPont (Wilmington, DE). Cisplatin was prepared as a 2 mg/ml stock solution in starvation medium (10 mM Tris-HCl, pH 7.4; Mochizuki *et al.,* 2008) and administered at a final concentration of 100 μg/ml to conjugating cells. MMS was appropriately diluted in starvation medium and added to conjugating cells at a final concentration of 4 mM (0.034%). Benomyl and nocodazole were applied at concentrations of 5 and 10 μg/ml, respectively. Stocks of 10 mg/ml DMSO were prepared by agitating for 1 h and then stored at −20°C. The kinase inhibitors caffeine or wortmannin were used at final concentrations of 10 mM and 2 μM, respectively, unless indicated otherwise. Caffeine was prepared as a 200 mM stock in starvation medium and kept at room temperature. As it tended to precipitate, it was heated to 37°C and agitated before use. Wortmannin was kept frozen as a 10 mM stock in DMSO. Effective concentrations for all drugs were empirically determined (data not shown).

All substances were added to cultures 110–120 min after mixing the cells. At this time, most cells have formed conjugating pairs while crescent elongation has not yet begun (Mochizuki *et al.,* 2008). In all cases, except where mentioned otherwise, the effect of the substances on MIC behavior was scored at t = 3.5 h after induction of meiosis, when most MICs have reached the stage of maximal elongation in untreated wild-type cells. The applied dosages of caffeine and wortmannin were not acutely toxic since cells survived this treatment for at least 8 h. Mock treatment with a 0.2% final concentration of DMSO (the solvent for wortmannin, benomyl, and nocodazole) had no visible effect on meiosis.

Cytological Preparation

For DAPI (4′6-diamidino-2-phenylindole) staining, cells were fixed by adding 250 μl of 10% Triton X-100 and 500 μl of 38% formaldehyde to a 5-ml cell suspension. Fixed cells were pelleted, postfixed with 4% paraformaldehyde + 3.4% sucrose, and applied to a slide (see Loidl and Scherthan, 2004). For Cna1p and γ-H2A.X immunostaining, cells were fixed by mixing 20 μl of partial Schaudin's fixative (saturated HgCl₂, ethanol 2:1) with a 5-ml cell suspension. After two washes with methanol, cells suspended in methanol were dropped on a slide (see Song *et al.,* 2007). For fluorescence in situ hybridization (FISH), 5 ml of cell suspension were centrifuged (3 min, 350 × g) and 1 ml of Carnoy's fixative (methanol-chloroform-acetic acid, 6:3:2) was added to the pellet. The fixed cells were washed with 70% ethanol, and cells suspended in 70% ethanol were dropped on a slide.

Fluorescence In Situ Hybridization

A FISH probe was produced by pooling PCR products generated from three neighboring sequences with a total length of 22.1 kb. Primers (see Supplemental Figure S1) were selected from the *T. thermophila* macronuclear genome sequence (Eisen *et al.,* 2006; http://www.tigr.org/tdb/e2k1/ttg/). The purified PCR products were labeled with Cy3 by nick translation. The probe and chromosomal DNA were denatured by hot formamide and hybridized for ~36 h at 37°C (for details see Loidl and Scherthan, 2004; Mochizuki *et al.,* 2008).

Cytological Staining and Microscopy

For indirect immunostaining, the following antibodies were used: rabbit anti-Cna1p (1:200; Cervantes *et al.,* 2006) and anti-γ-H2A.X [1:200 purified mouse monoclonal anti-H2A.X phosphorylated (Ser139) antibody Clone 2F3; BioLegend, San Diego, CA]. Slides were washed with 1× phosphate buffered saline (PBS) and 1× PBS + 0.05% Triton X-100 for 10 min each. Primary antibodies were applied to the preparations under a coverslip for ~3 h at room temperature. After a series of washes as above, secondary antibodies were applied in the same way. After a final round of washes, slides were mounted in Vectashield anti-fading agent (Vector Laboratories, Burlingame, CA) supplemented with 1 μg/ml DAPI under a coverslip.

Fluorescence was elicited with appropriate filter sets in an epifluorescence microscope. 3D image stacks were recorded using a CCD camera and Meta-Vue software (Universal Imaging, Downingtown, PA). The images were deconvolved and projected with AutoDeblur (AutoQuant Imaging, Watervliet, NY) and ImageJ (Wayne Rasband, NIH; http://rsb.info.nih.gov/ij/) software (Mochizuki *et al.,* 2008).

RESULTS

Elongation and Chromosomal Orientation in the Wild-Type MIC

To put MIC behavior under various experimental conditions in context, the situation in untreated wild type is briefly recapitulated for reference (see also Mochizuki *et al.,* 2008): Shortly after induction of meiosis by mixing cells of different
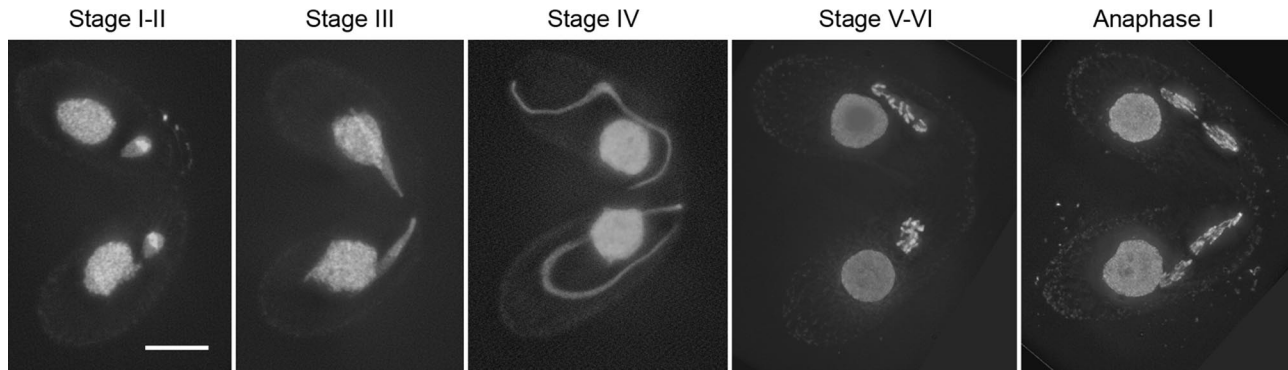
Figure 1. Meiotic MIC development in wild-type *Tetrahymena*. Stages are numbered according to Sugai and Hiwatashi (1974). On initiation of meiosis in paired cells of different mating types, MICs change from being round (stage I) to being egg-shaped (stage II). Further elongation leads to barrel- to spindle-shaped nuclei (stage III) and to long threads "crescents" (stage IV). The MICs shorten again while chromatin condenses into distinct entities (stage V), which finally emerge as five bivalents (stage VI). The nuclei then undergo a canonical first and second (not shown) division. DAPI staining. Bar, 10 μm.

mating types, round MICs started to elongate and assumed the shape of an egg, a barrel, a spindle, and finally a long wound thread (Figure 1). These shapes are also referred to as stages I–IV (Sugai and Hiwatashi, 1974). Centromeres (as identified by their association with the histone variant Cna1p; see Cervantes *et al.,* 2006; Cui and Gorovsky, 2006) were clustered on one side of the MIC when it was still round. This presumably reflects the mitotic Rabl orientation of chromosomes, i.e., the localization of centromeres and telomeres at opposite poles (Mochizuki *et al.,* 2008 and references therein). In egg- to spindle-shaped MICs, this clustering was lost transiently but during further elongation centromeres assumed increasingly terminal positions. In the tip of fully elongated crescents, centromeres mostly reassembled in a single spot (Figure 2a). Concomitantly with elongation, pairing of homologous loci (as visualized by FISH) occurred (Figure 3, a–e). After maximal elongation, the MICs shortened again and transformed into condensed bivalents (Figure 1). Immunostaining of phosphorylated histone H2A.X (γ-H2A.X) and recombination protein Rad51 has provided evidence that DSB formation and repair are ongoing in MICs during elongation (Loidl and Scherthan, 2004; Song *et al.,* 2007; Mochizuki *et al.,* 2008).

UV and MMS Induce MIC Elongation in the spo11Δ Mutant

We have previously shown that in addition to its conserved role in DSB formation, Spo11p is required for the full elongation of meiotic MICs in *Tetrahymena*. However, elongation in a *spo11*Δ mutant was restored by the DSB-inducing drug cisplatin (Figure 4, a and b), which led to the conclusion that meiotic DSBs rather than a function of Spo11p unrelated to DSBs promote MIC elongation (Mochizuki *et al.,* 2008). Since exposure to cisplatin is a chronic treatment that affected cells in repair-competent and -incompetent stages alike, we repeated DSB induction by acute γ-irradiation of conjugating cells at t = 120 min after induction of meiosis with a dosage of 5000 rad. At this time, the majority of cells start to develop DSBs in the wild type. Indeed, exposure of cells to γ-radiation reinduced MIC elongation in the *spo11*Δ (Figure 4, a and b).

We next wanted to know whether other DNA-damaging agents would similarly trigger MIC elongation. To this end, we exposed DSB-deficient meiotic cells to UV-C radiation, the primary effect of which is not DSB formation (Marti *et al.,* 2006). We found that 254 nm UV (UV-C) at doses as low as 20 J/m² efficiently induced crescents in *spo11*Δ cells (Figure

4, a and b). At t = 3.5 h post-mixing, when stage IV crescents were most abundant in the wild type, almost as many irradiated *spo11*Δ conjugants displayed crescents, whereas no such nucleus appeared in the untreated *spo11*Δ control (Figure 4b).

To determine whether MIC elongation was caused by UV-induced DNA lesions, we immunostained nuclei for the phosphorylated histone variant H2A.X (γ-H2A.X). γ-H2A.X is considered to be an indicator of the occurrence of meiotic DSBs (Mahadevaiah *et al.,* 2001; Song *et al.,* 2007), but there are recent reports on DSB-independent H2A.X phosphorylation (Marti *et al.,* 2006; Hanasoge and Ljungman, 2007; Ismail and Hendzel, 2008). γ-H2A.X forms patches in elongating wild-type MICs (Figure 5a), whereas it is absent from MICs in the *spo11*Δ mutant (Figure 5e; see also Mochizuki *et al.,* 2008). γ-H2A.X immunostaining was restored by a dose of 20 J/m² UV (Figure 5g). About one-third of fully elongated MICs lacked staining 90 min after exposure to UV, but all MICs (and MACs) displayed γ-H2A.X foci 15 and 60 min after exposure. This means that UV-induced lesions were partially repaired by the time MICs were fully elongated, but H2A.X phosphorylation and MIC elongation were both triggered by DNA lesions. However, the fact that MICs elongate normally in a mutant with nonphosphorylatable H2A.X (Song *et al.,* 2007) indicates that they do not depend on each other.

To evaluate the possibility that MIC elongation is caused by DNA lesions other than DSBs, we treated the *spo11*Δ mutant with the alkylating agent MMS. Like UV, MMS does not directly cause DSBs in vivo (Lundin *et al.,* 2005). Indeed, after treatment with 4 mM (0.034%) MMS, MIC elongation was observed (Figure 4, a and b). The failure to detect chromosome fragmentation by pulsed-field electrophoresis (unpublished observation), together with published evidence of the non-DSB nature of UV-induced lesions (see *Discussion*), suggest that DSBs may be rare after a UV dosage of 20 J/m², which is sufficient to induce MIC elongation.

In Caffeine- and Wortmannin-treated Meioses, MICs Do Not Fully Elongate

Since the restoration of full MIC elongation by different agents suggested that DSBs and possibly also DNA lesions other than DSBs can trigger full MIC elongation, we wanted to know how a DNA-damage signal for MIC elongation is conveyed. The phosphatidylinositol 3-kinase (PI3K)-related sensor kinases ATM and ATR are key players in the signal-
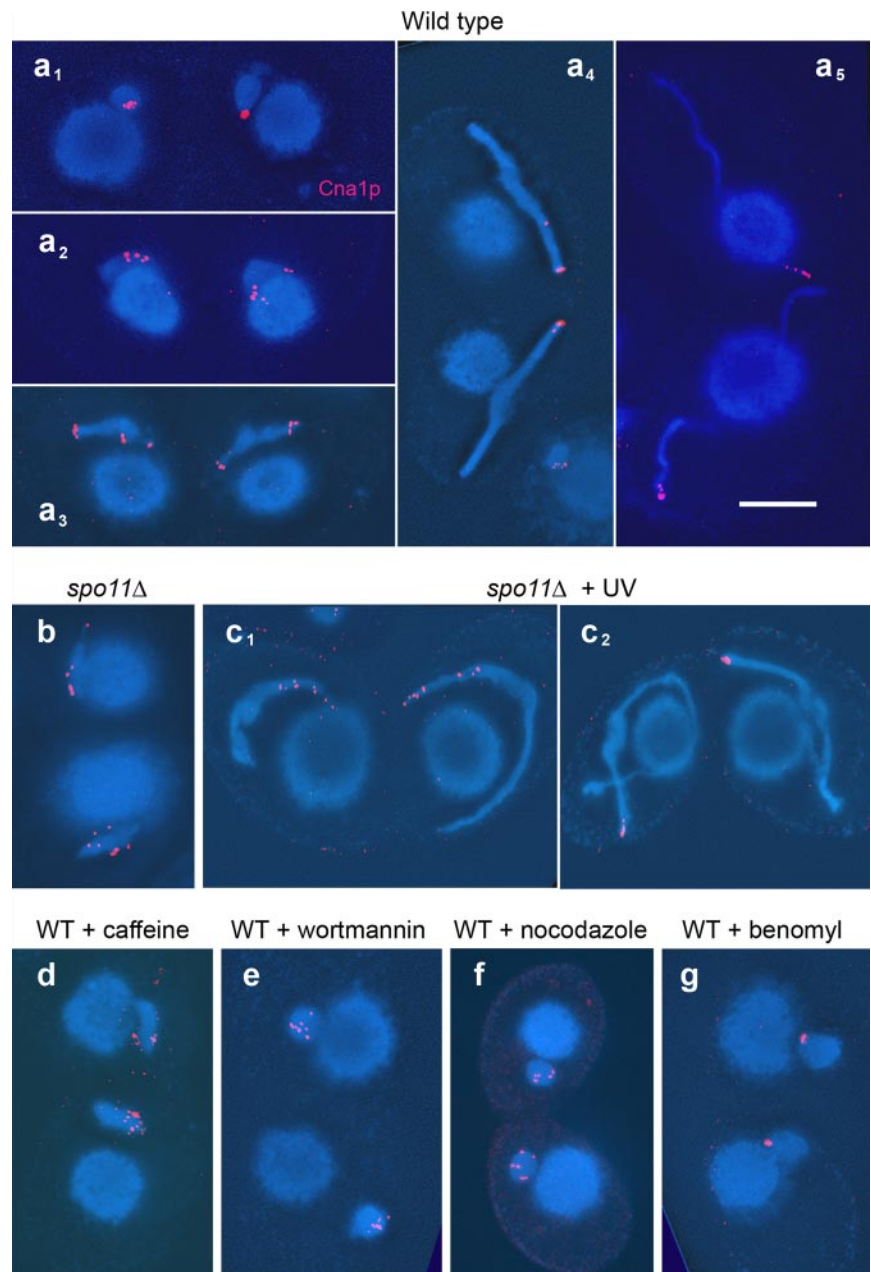
Figure 2. Immunostaining of centromeric histone variant Cna1p (red). (a) Wild-type (WT). In round, early meiotic MICs of untreated wild type, centromeres are grouped together in a small region (a1). As MIC elongation begins, this grouping is lost (a2 and a3), but centromeres reassemble again at one tip of the MIC while elongation proceeds (a4 and a5). (b) In the *spo11Δ* mutant, centromere rearrangement arrests at the dispersed stage, but UV treatment restores not only MIC elongation but also wild-type internal organization, as suggested by the clustering of centromeres (c1 and c2). Kinase inhibitors caffeine (d) and wortmannin (e) prevent both centromere clustering and MIC elongation. Also in the presence of the MT inhibitor nocodazole, centromere clustering fails (f). The MT inhibitor benomyl permits centromere clustering in most MICs although MIC elongation does not take place (g). Note that in elongating MICs (of WT and *spo11Δ* + UV), where centromeres are not yet completely clustered, there is always at least one Cna1p dot at the very tip. This suggests that the pushing of centromeres away from the telomeric pole of the MIC mediates its stretching. Bar, 10 μm.

ing of induced DNA damage and self-inflicted DNA cuts in vegetative and meiotic cells (Richardson *et al.*, 2004; Bassing and Alt, 2004; Hunter, 2008). They are recruited by the MRX/MRN complex and possibly also by yet unknown factors to the sites of damage and phosphorylate a host of targets (Kurz and Lees-Miller, 2004). It was previously reported that ATM and ATR kinases are inhibited by relatively high doses of caffeine (Cortez, 2003) and by wortmannin (Sarkaria *et al.*, 2008). We, therefore, treated conjugating wild-type cells with these two agents.

In the presence of caffeine, MIC elongation did not proceed beyond the spindle-shaped stage (Figure 4c, Supplemental Table S2), i.e., it arrested at a similar stage as the *spo11Δ* mutant. Wortmannin showed a similar effect at a final concentration of 2 μM (Figure 4c; Supplemental Table S2). Some MICs were slightly oblong and others considerably enlarged and round, but none became elongated to the

extent of untreated MICs (Figure 4c). We found that also the response to UV-induced lesions in *spo11Δ* cells is wortmannin-sensitive (data not shown).

While both kinase inhibitors efficiently prevented meiotic MIC elongation, other aspects of meiosis appeared to continue, since Rad51p was expressed (data not shown). Neither caffeine nor wortmannin had a toxic effect on vegetatively growing cells although locomotion was slowed down with the latter–upon removal of the agents the cells continued normal growth. However, meiosis did not resume normally. At least in part, this could be due to the fact that caffeine and wortmannin caused opening of the aperture between the conjugating cells, leading to the migration of both MACs and MICs between the partners or even the complete fusion of the cells (Figure 4c).

To test the hypothesis that the effective target of the inhibitors is ATM or ATR rather than PI3Ks proper, we per-
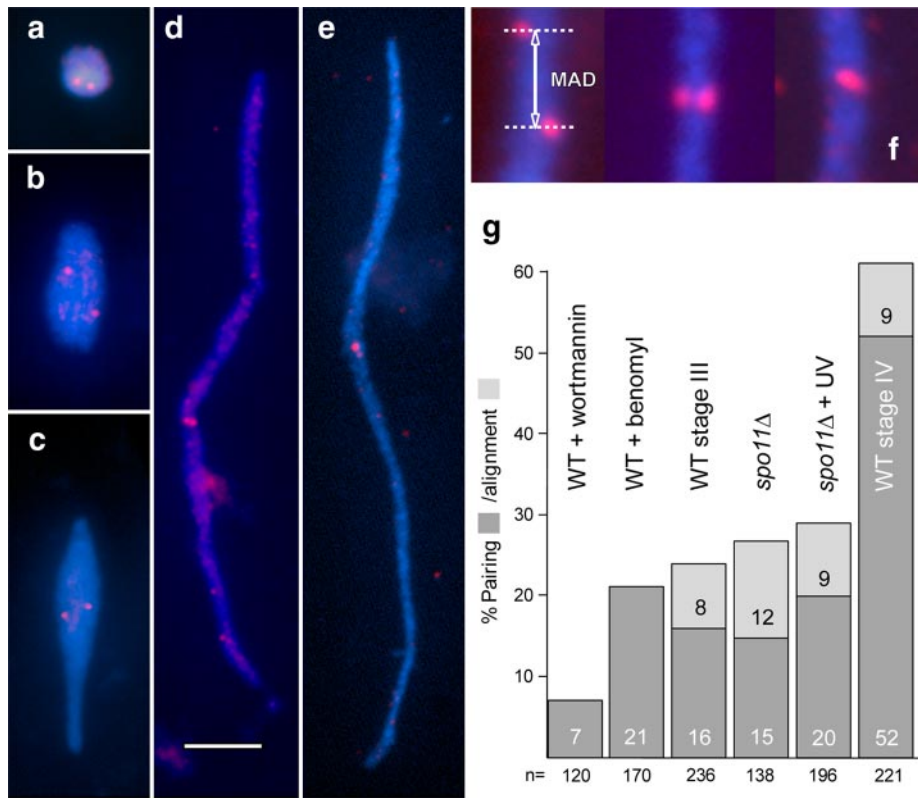
Figure 3. Examples of meiotic MICs (a, stage I; b, stage II; c, stage III; d and e, stage IV) with FISH signals (red) representing unpaired loci in a–d and paired loci in e. The FISH probe (see Supplemental Figure S1) was selected so that it localizes to the middle of crescents. Because in the mature crescent (stage IV) all telomeres congress on one end (Mochizuki *et al.,* 2008) and the centromeres on the opposite end (see Figure 2a), a locus found in the middle of a crescent must be situated in an intercalary position of a chromosome arm. This region has the advantage that its pairing behavior is largely independent of seeming pairing conferred by the clustering of centromeres and telomeres. Carnoy fixation removes MICs from the cells, and they become flattened and straightened out on the slide, which facilitates the quantitative evaluation of FISH signals. Bar, 5 μm. (f) Examples of misaligned, aligned, and paired loci within crescents. The misalignment distance (see text) was measured as indicated (MAD). (g) Pairing and alignment of FISH signals at different MIC elongation states. Pairing is infrequent in enlarged but round MICs of wortmannin-treated wild type (WT). After benomyl treatment, paring of the intercalary locus is only slightly increased despite centromeres becoming

clustered in one spot at the periphery of the nucleus (see Figure 2g). The concept of aligned signals as used here (f) is not applicable to round nuclei. Also in slightly elongated nuclei (*spo11Δ* and WT stage III) pairing is still low. Notably, despite full nuclear elongation in the UV-treated *spo11Δ* mutant (see Figure 4), pairing does not reach the level of WT stage IV (n = number of nuclei inspected).
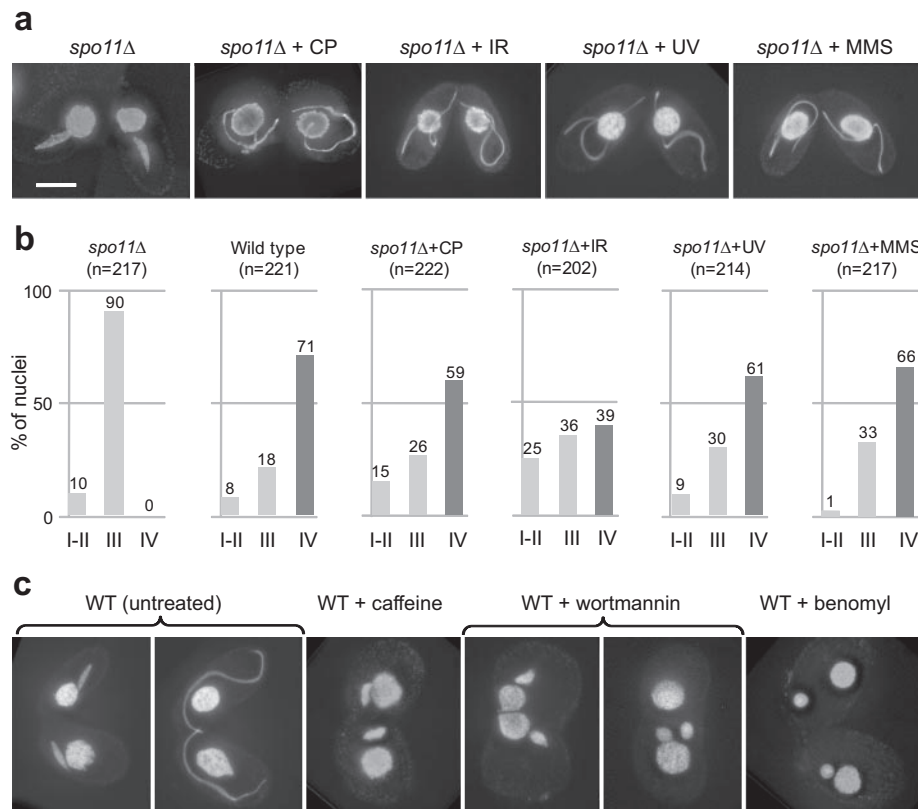

Figure 4. MIC behavior under various conditions. (a) In the *spo11Δ* mutant, MIC elongation arrests at a spindle-shaped stage, but treatment with cisplatin (CP), ionizing radiation (IR), UV, or MMS restores full elongation (crescent). (b) MIC shapes 3.5 h after induction of meiosis. Relative frequencies of round and egg-shaped (stage I-II), spindle-shaped (stage III), and full-crescent (stage IV) MICs are shown. Although in the untreated *spo11Δ* strain MICs arrest early in elongation and the frequency of fully elongated, crescent-shaped stage IV MICs is zero, treatment with cisplatin (CP), ionizing radiation (IR), UV, or MMS restores this class of nuclei to almost wild-type levels. The sample size n of nuclei scored in each experiment is given in brackets. (c) In the wild type (WT), meiotic MICs change their shape from spindle-shaped to full-crescent. However, elongation is suppressed by treatment with the kinase inhibitors caffeine or wortmannin or with the microtubule inhibitor benomyl. (a and c) DAPI staining. Bar, (a and c) 10 μm.
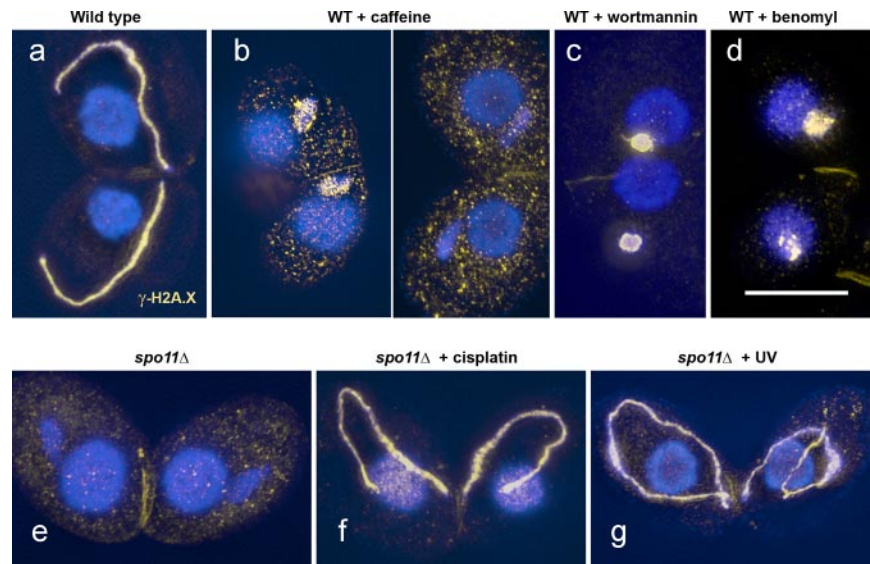
Figure 5. Induction of γ-H2A.X signals in meiotic MICs. In wild type, strong γ-H2A.X immunostaining (orange) is detected in elongated MICs (a). After treatment with caffeine, H2A.X phosphorylation is partially suppressed (two examples with different intensities of γ-H2A.X labeling shown in panel b, whereas upon wortmannin treatment labeling is always strong (c). Also after benomyl (d) and nocodazole (not shown) treatment, γ-H2A.X signals are found, suggesting that other aspects of meiosis progress despite the failure of MICs to elongate. In the *spo11Δ* mutant, γ-H2A.X labeling is not observed (e). Cisplatin restores strong γ-H2A.X labeling in the mutant (f). Also UV-radiation induces γ-H2A.X foci in the mutant (g), but they become fewer and disappear ca. 90 min after the treatment. Bar, 10 µm.

formed a dose response experiment with wortmannin at concentrations of 2 µM, 1 µM, 500 nM, and 250 nM. It has been shown that the PI3K-related kinases ATM and particularly ATR are inhibited by wortmannin only at significantly higher concentrations than PI3Ks (Sarkaria *et al.,* 1998; Liu *et al.,* 2005; Knight *et al.,* 2006). Accordingly, wortmannin at 250 nM impaired nuclear degradation in *Tetrahymena* (Yakisich and Kapler, 2004), but it inhibited the—presumably—ATR-dependent intra-S-phase DNA damage checkpoint response only at 2 µM (Yakisich *et al.,* 2006). Here, we observed that concentrations below 2 µM did not effectively inhibit MIC elongation (Supplemental Table S3), which is consistent with the suppression of ATM or ATR activity.

Our results show that two different kinase inhibitors inhibit MIC elongation at concentrations similar to those previously reported to affect ATM and ATR. This suggests that DNA lesions–most likely Spo11p-induced DSBs in untreated wild-type cells–trigger full MIC elongation via a phosphokinase signal transduction pathway involving ATM and/or ATR homologues. As expected of an ATM/ATR inhibitor, caffeine strongly reduced γ-H2A.X immunostaining. Although in some caffeine-treated meiotic MICs weak staining was observed (Figure 5b), comparable staining was also present in nonmeiotic MICs (Supplemental Figure S4), suggesting that this staining is not specific to meiotic DNA damage. Notably, wortmannin treatment did not fully suppress H2A.X phosphorylation (Figure 5c; Supplemental Figure S4). Thus, a reduced activity of the potential kinase(s) upon which MIC elongation is no longer permitted may be still sufficient for H2A.X phosphorylation. Another possible explanation is that the signaling cascades from DNA lesions to H2A.X phosphorylation on the one hand and to MIC elongation on the other hand are different.

Knockout of ATR1 Suppresses MIC Elongation

A Tetrahymena orthologue of ATR (TTHERM_01008650) but not of ATM has been identified by a bioinformatics search (Yakisich *et al.,* 2006), making the former the likely target of chemical inhibition.

To further strengthen the supposition that ATR is involved in the signaling that triggers MIC elongation, we produced macronuclear knockout strains of ORF TTHERM_01008650 (in the following called *ATR1*). Clones lost vigor under strongly se-

lective growth conditions (paromomycin concentrations above ~4 mg/ml) when a high proportion of wild-type *ATR1* copies became replaced by the knockout construct carrying the resistance marker. Cells often featured tiny and/or weakly staining MICs (data not shown), which could indicate chromosome loss. This suggests that ATR is important for vegetative growth. Nevertheless, practically complete knockout of the ~45 macronuclear *ATR1* copies could be attained (Figure 6a), and *atr1Δ* cells conjugated efficiently. Fully elongated MICs were almost completely missing. In one experiment, 86.5% (n = 200) of MICs were arrested at a spindle-shaped stage (Figure 6b) 3.5 h after induction of meiosis, resembling those found in *spo11Δ* cells (Figure 4a). In addition, some irregularly shaped MICs occurred, which also parallels the situation in *spo11Δ*, and a mere 0.5% of MICs were fully elongated (stage IV) crescents (Supplemental Table 2). These fully elongated MICs may be due to the restoration of a sufficient number of wild-type *ATR1* copies in the MACs of individual cells due to random assortment and a strong selection for the presence of ATR during vegetative growth. Conjugation of two different *atr1* knockout lines gave similar results. (It should be noted that the meiotic defect in *atr1Δ* cells is not caused by the failure to undergo DSBs or other DNA lesions, since MIC elongation was not restored upon treatment with cisplatin or UV.) Altogether, these observations strongly support the involvement of ATR in MIC elongation in response to DSBs.

In contrast to caffeine- and wortmannin-treated MICs, γ-H2A.X immunostaining was almost completely eliminated in *atr1Δ* MICs. Only 0.5% of stage III-like MICs (n = 200) displayed staining, and the rare stage IV escapers (see above) were γ-H2A.X-positive.

Centromere Clustering and MIC Elongation Are Jointly Regulated

As already mentioned, centromeres are clustered in MICs at the beginning of meiosis, disperse during the MIC elongation phase and converge at one (the telomere-distal) tip in the full crescent (Figure 2a). In the *spo11Δ* mutant, spindle-shaped MICs persist with dispersed centromeres (Figure 2b; Mochizuki *et al.,* 2008) before they take a shortcut into aberrant meiotic divisions.

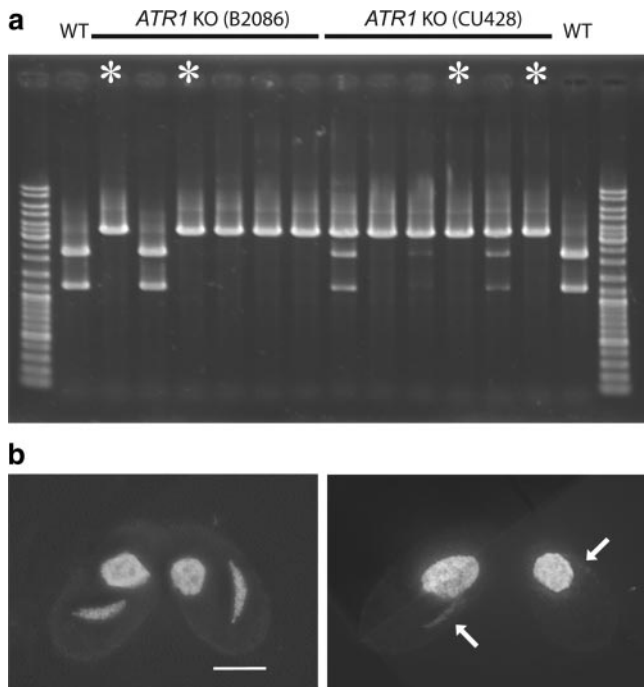We wanted to know whether UV radiation restores centromere clustering in the *spo11Δ* mutant. Indeed, similar to

Figure 6. Genotype and phenotypes of macronuclear *ATR1* knock-out cells. (a) PCR with primers flanking the *ATR1* locus demonstrates the elimination of wild-type copies of the gene in numerous knockout strains. To differentiate the equal-sized wild-type and knockout PCR products, they were digested with PvuII, which cuts only the wild-type product. The lack of detectable wild-type PCR products in several of the strains suggests the loss of wild-type copies also from the MIC and provides additional evidence for micronuclear chromosome loss as a consequence of ATR depletion (see text). Asterisks indicate DNA of the strains that were used. (b) Examples of DAPI-stained conjugating *atrΔ* cells. MIC elongation arrests with stage III-like nuclei resembling those found in *spo11Δ* cells. The right panel shows cells with weakly stained MICs (arrows) that probably suffered chromosome loss. Bar, 10 μm.

the wild type, Cna1p spots congressed at the tip of full crescents (Figure 2c). This means that in addition to MIC elongation, internal reorganization of MICs is induced by UV irradiation. In contrast, in the nonelongating MICs of caffeine- and wortmannin-treated wild-type meioses, centromeres remained dispersed (Figure 2, d and e).

This suggested that the failure to cluster was due to the failure of MICs to elongate. To test this hypothesis, we prevented MIC elongation in wild type with the microtubule (MT) inhibitors nocodazole and benomyl. MIC elongation depends on intranuclear MTs (Wolfe *et al.,* 1976), and MT inhibitors can prevent the elongation of MICs (Kaczanowski *et al.,* 1985). In the presence of inhibitors, the MICs somewhat enlarged but remained spherical (Supplemental Table S2), while the presence of γ-H2A.X suggested that DSBs were created (Figure 5d). Indeed, nocodazole completely suppressed the merging of Cna1p dots into a single cluster (Figure 2f). Surprisingly, under the influence of benomyl, centromeres managed to cluster in the majority of meiotically advanced MICs (Figure 2g). It is possible that this is due to a lower efficiency of this drug. Nevertheless, the failure of centromeres to cluster in nocodazole-treated MICs as in the other cases of aborted MIC elongation rather suggests that centromere clustering and MIC elongation are not functionally separable, and their sensitivity to caffeine and wortmannin indicates that both processes depend on DNA

damage signaling. It is conceivable that the elongation of MTs pushes centromeres and telomeres apart and at the same time stretches the MIC.

MIC Elongation Is Not Sufficient for Homologous Chromosome Pairing

The confinement of chromosomes within the tubular crescent has been proposed to promote the juxtaposition of homologous loci and to support meiotic homologous pairing (Mochizuki *et al.,* 2008). In addition, full pairing might require the stabilization of homologous links by the interaction of DSB sites with homologous chromosomal loci, as was found in many organisms (Peoples-Holst and Burgess, 2005; Zickler, 2006). Here we assessed the influence of MIC shapes on homologous associations of a FISH-marked chromosomal locus. We compared pairing in full (stage IV) crescents of the wild type, in UV-irradiated *spo11Δ* where MICs formed full crescents yet DSBs were likely missing, in MICs of wild-type stage III and of *spo11Δ*, which were only partially elongated, and, finally, in wortmannin-treated wild type where MICs increased in volume but did not elongate, although other aspects of meiosis were ongoing. We selected a FISH probe for a region approximately halfway between the centromeric and the telomeric end of the elongated MIC (Figure 3; Supplemental Figure S1) to reduce the influence of centromere and telomere clustering on the juxtapositioning of homologous regions. If two homologous FISH signals merged into one, the locus was scored as paired, if the signals were separate but occupied similar positions along the crescent, they were scored as aligned, and otherwise as misaligned (Figure 3f). In the latter case, the lengthwise distance between the signals was measured to quantify the misalignment (Figure 3f).

Pairing was least frequent (7%) in wortmannin-treated wild-type MICs that remained spherical, whereas 52% of stage IV crescents of the wild type had the intercalary locus paired (Figure 3g). The somewhat higher pairing frequencies reported previously for wild type (Mochizuki *et al.,* 2008) were likely due to the study of distal chromosomal loci whose juxtapositioning is promoted by the clustering of telomeres. In wild-type stage III and in *spo11Δ* slightly elongated MICs, pairing was more frequent (16 and 15%, respectively) than in the wortmannin MICs. A similar pairing frequency (21%) was observed for benomyl-treated MICs (Figure 3g). This suggests that the clustering of centromeres, which was frequently observed in the presence of this drug (see above), was not sufficient to bring homologous loci together.

Interestingly, pairing in *spo11Δ* UV-induced full crescents (20%) was not significantly increased compared with the untreated *spo11Δ* mutant. This indicates that also MIC elongation is not sufficient for achieving a wild-type level of homologous chromosome pairing. Limited colocalization of homologous loci in UV-irradiated MICs is also reflected by a mean lengthwise separation distance between unpaired signals (misalignment distance; see Figure 3f) of 1.5 μm (SD = 1.2, n = 196) in the *spo11Δ* + UV crescents compared with only 0.7 μm (SD = 0.7, n = 221) in the wild type. This suggests that even though homologous chromosomes become arranged in parallel tracks inside the crescent, corresponding loci can still be separated by considerable lengthwise distances, but once recombination is initiated at several sites along a chromosome pair in the wild type, chromosome movement is frozen. Lengthwise mobility of chromosome regions may be a mechanism which allows homologous loci to search for each other (see *Discussion*).

As expected from the failure of UV irradiation to induce pairing in a *spo11Δ* mutant, bivalent formation was not restored by either 20 or 80 J/m² UV. Irradiated cells only had univalents 4.5 h after meiotic induction that resembled those of untreated *spo11Δ* (Supplemental Figure S5). Bivalent formation has been found in *spo11* mutants of *Caenorhabditis elegans* and *Arabidopsis* after exposure to γ-radiation and cisplatin, respectively (Dernburg *et al.*, 1998; Penkner *et al.*, 2007; Sanchez-Moran *et al.*, 2007). However, we failed to observe bivalents under our conditions of γ-irradiation (Supplemental Figure S5), and cisplatin-treated meioses failed to exit from the crescent altogether (data not shown). It is conceivable that exit from this stage only occurs when meiotic DNA lesions are cured, but is impeded because of ongoing assault by the drug.

DISCUSSION

Induction of MIC Elongation in the spo11Δ Mutant by DNA-damaging Agents

In meiosis deprived of Spo11p, MICs do not fully elongate, but crescent formation can be restored by cisplatin-treatment (Mochizuki *et al.*, 2008). Spo11p is a DNA endonuclease that induces programmed DSBs that are essential for crossing over and bivalent formation (see Keeney, 2007). Also cisplatin induces DSBs, which have been shown to stimulate meiotic recombination (Hanneman *et al.*, 1997; Sanchez-Moran *et al.*, 2007). It was therefore concluded that in wild-type meiosis Spo11p-dependent DSBs serve as a signal for MIC elongation. In the absence of Spo11p and MIC elongation, the subsequent steps of meiosis follow with little if any delay. Therefore, DSBs are not a signal for meiosis progression. They may, however, induce the formation of the crescent to bring about homologous pairing, thus allowing recombinational repair of DSBs via the homologue.

Here we elicited MIC elongation in the *spo11Δ* mutant by a variety of genotoxic agents, namely MMS, ionizing radiation and short-wave UV. We concentrated on the study of the effects of UV, since acute irradiation unlike chronic chemical treatment, which also affects cells at nonmeiotic repair-incompetent stages, is less likely to cause side effects. Moreover, UV causes DNA lesions that are different from those resulting from ionizing radiation and cisplatin.

The primary defect caused by UV-C radiation is base dimerization, which is repaired by base excision repair. It has been calculated that DSBs as a direct consequence of UV-C would be extremely unlikely as they would only occur at overlapping excision repair sites (Marti *et al.*, 2006). These authors also found that UV and ionizing radiation–induced lesions in human fibroblasts did not lead to H2AX phosphorylation by the same kinases and hence concluded that the former were not DSBs. Like UV, MMS does not directly cause DSBs in vivo (Lundin *et al.*, 2005). Yet we were able to induce MIC elongation in *spo11Δ* by both treatments, which raises the possibility that it may be triggered also by DNA lesions other than DSBs. Whereas previous studies had suggested that γ-H2A.X is not induced by DNA lesions other than DSBs (for review see Ismail and Hendzel, 2008), there is now accumulating converse evidence (Smart *et al.*, 2008). In particular, it was noted that γ-H2AX induced by UV in G_1 is not due to DSBs (Marti *et al.*, 2006; Hanasoge and Ljungman, 2007; Ismail and Hendzel, 2008). Therefore, the induction of γ-H2A.X foci by UV in *Tetrahymena* is not a sure sign of the occurrence of DSBs.

A possible alternative to MIC elongation being caused by non-DSB DNA damage is that UV-induced DNA lesions are converted to DSBs during meiosis. Following base damage by UV there is a base excision over ~30 nucleotides. Transient single-strand DNA (ssDNA) tracts could then be attacked by single-strand endonucleases (such as the MRX/MRN complex; see Kanaar and Wyman, 2008), which are part of the meiotic recombination machinery, and be converted to DSBs.

MIC Elongation Is Elicited by a Caffeine- and Wortmannin-sensitive Signal Response to DNA Damage

Whatever kind of DNA damage causes MIC elongation, it is sensed by a signaling pathway that is sensitive to caffeine and wortmannin as these substances phenocopy the MIC elongation defect seen in *spo11Δ* meiosis. In vivo studies in human cell lines suggest that caffeine can block cell cycle checkpoint responses without inhibiting ATM or ATR activation (Cortez, 2003). On the other hand, Yakisich *et al.* (2006) found evidence for a caffeine-sensitive intra-S-phase checkpoint activated by an ATR-like protein kinase (TTHERM_01008650) in *Tetrahymena*. Notably, Tif1p, a likely factor in the presumed checkpoint pathway, may also have a role in the response to meiotic DSBs since the *TIF1*-deficient partner in mating pairs of wild-type and *tif1* mutant cells displayed reduced crescent formation (Morrison *et al.*, 2005). It has been reported that wortmannin at low doses inhibits PI3K-dependent MT-mediated processes in a *Tetrahymena* strain with attenuated β-tubulin (Smith *et al.*, 2004). Hence, it is possible that caffeine and wortmannin prevent MIC elongation via a PI3K signaling pathway acting on MTs. However, our observation of the sensitivity of MIC elongation to wortmannin only at high doses (at which it is known to inhibit PI3k-like kinases) rather suggests that MIC elongation is triggered by sensing meiotic DNA lesions via a pathway involving the ATR orthologue.

The possible involvement of ATR is most convincingly shown by the deletion of ORF TTHERM_01008650 (here called *ATR1*) encoding *Tetrahymena*'s ATR orthologue. In conjugating *atr1* knockout strains, stage IV MICs were absent which strongly supports a role of ATR in meiotic MIC elongation. However, *atr1* knockout strains also showed growth defects and signs of micronuclear chromosome loss. Therefore, it cannot be excluded that the failure of MICs to fully elongate is due to the generally weakened constitution and micronuclear anomalies displayed by these strains.

The failure of *atr1Δ* nuclei to undergo both full MIC elongation and H2A.X phosphorylation whereas wortmannin treatment suppressed only the former suggests a different ATR dosage requirement by the two processes. Alternatively it is possible that wortmannin inhibits (primarily) a kinase downstream of ATR, which is involved in MIC elongation but not in H2A.X phosphorylation. In any case, γ-H2A.X immunostaining in MICs whose elongation was inhibited by wortmannin indicates that H2A.X phosphorylation is not a signal for MIC elongation. This is consistent with the observation by Song *et al.* (2007) that MIC elongation occurs normally in a mutant with nonphosphorylatable H2A.X. Together, these results suggest that the pathways leading to MIC elongation and to H2A.X phosphorylation overlap but are not identical.

The Tetrahymena Crescent Shows Structural Features of the Bouquet But Is Regulated Differently

The bouquet has been implicated in various aspects of homologous pairing (for review see Zickler, 2006). While it is not absolutely required for either homologous pairing or synapsis, it makes both processes faster and more efficient (Harper *et al.*, 2004). As alternative bouquet functions unre-

lated to pairing, the resolution of chromosomal interlockings and the destabilization of ectopic interactions have been invoked (Zickler, 2006). Recently, it was found that in fission yeast the bouquet helps form the meiotic spindle, and is therefore critical to chromosomal division (Tomita and Cooper, 2007).

Meiosis in mice lacking Spo11 or ATM is arrested in the bouquet stage (Liebe *et al.*, 2006), which is also reflected by enduring telomere clustering during spermatogenesis in an ATM knockout (Pandita *et al.*, 1999). Similarly, telomere clustering persists in *spo11* mutants of *Sordaria* and budding yeast (Trelles-Sticken *et al.*, 1999; Storlazzi *et al.*, 2003). This suggests that in mice, and possibly in other organisms as well, ATM regulates the exit from the bouquet in response to the processing of recombination intermediates (Storlazzi *et al.*, 2003; Scherthan, 2006).

In *Tetrahymena*, in contrast, the establishment of the crescent with its bouquet-like chromosome arrangement seems to depend on DNA lesions (most likely DSBs in the wild-type situation) and their signaling to the cell cycle. This raises the possibility that the bouquet and the crescent are different devices. We have not yet been able to identify any *Tetrahymena* homologues of genes that are known for their conserved role in bouquet formation. Future studies of MIC reorganization will reveal whether the bouquet and the crescent are homologous structures or analogous designs.

There is strong evidence that the meiotic MIC stretches and moves by the elongation of intranuclear MTs (Wolfe *et al.*, 1976; Kaczanowski *et al.*, 1985). Our observation that the tip of an elongating MIC is always occupied by at least one Cna1 spot (see Figure 2) suggests that centromeres are not transported to the tip of the elongated crescent in an independent subsequent move, but that they migrate at the front of the elongating MIC. This suggests a model where both the tip of the MIC and centromeres are pushed by MTs emanating from the pole where the telomeres are anchored.

While in all cases of meiotic pairing, a movement of chromosomes is generated inside the nucleus that brings about transient random contacts during which homology can be tested (see Loidl, 1990), it may be achieved by different mechanisms. In the classical bouquet (and probably also in *C. elegans* transition zone nuclei), movement is created by extranuclear actin that is transmitted by transmembrane proteins (Koszul *et al.*, 2008). In the *Schizosaccharomyces pombe* horsetail, it is probably the oscillation of the nucleus between the cell poles that confers the stirring of the nuclear contents (Yamamoto and Hiraoka, 2001). In *Tetrahymena*, it may be MIC elongation by intranuclear MTs that causes allelic loci to collide and establish homologous contacts.

ACKNOWLEDGMENTS

REFERENCES

Alsheimer, M., von Glasenapp, E., Hock, R., and Benavente, R. (1999). Architecture of the nuclear periphery of rat pachytene spermatocytes: distribution of nuclear envelope proteins in relation to synaptonemal complex attachment sites. Mol. Biol. Cell *10*, 1235–1245.

Bass, H. W., Riera-Lizarazu, O., Ananiev, E. V., Bordoli, S. J., Rines, H. W., Phillips, R. L., Sedat, J. W., Agard, D. A., and Cande, W. Z. (2000). Evidence for the coincident initiation of homolog pairing and synapsis during the telomere-clustering (bouquet) stage of meiotic prophase. J. Cell Sci. *113*, 1033–1042.

Bassing, C. H., and Alt, F. W. (2004). The cellular response to general and programmed DNA double strand breaks. DNA Repair *3*, 781–796.

Cassidy-Hanley, D., Bowen, J., Lee, J. H., Cole, E., VerPlank, L. A., Gaertig, J., Gorovsky, M. A., and Bruns, P. J. (1997). Germline and somatic transformation of mating *Tetrahymena termophila* by particle bombardment. Genetics *146*, 135–147.

Cervantes, M. D., Xi, X., Vermaak, D., Yao, M. C., and Malik, H. S. (2006). The CNA1 histone of the ciliate *Tetrahymena thermophila* is essential for chromosome segregation in the germline micronucleus. Mol. Biol. Cell *17*, 485–497.

Collins, K., and Gorovsky, M. A. (2005). *Tetrahymena thermophila*. Curr. Biol. *15*, R17–R18.

Cortez, D. (2003). Caffeine inhibits checkpoint responses without inhibiting the ataxia-telangiectasia-mutated (ATM) and ATM- and Rad3-related (ATR) protein kinases. J. Biol. Chem. *278*, 37139–37145.

Cui, B. W., and Gorovsky, M. A. (2006). Centromeric histone H3 is essential for vegetative cell division and for DNA elimination during conjugation in *Tetrahymena thermophila*. Mol. Cell. Biol. *26*, 4499–4510.

Dernburg, A. F., McDonald, K., Moulder, G., Barstead, R., Dresser, M., and Villeneuve, A. M. (1998). Meiotic recombination in *C. elegans* initiates by a conserved mechanism and is dispensable for homologous chromosome synapsis. Cell *94*, 387–398.

Eisen, J. A., *et al.* (2006). Macronuclear genome sequence of the ciliate *Tetrahymena thermophila*, a model eukaryote. PLoS Biol. *4*, 1621–1642.

Hanasoge, S., and Ljungman, M. (2007). H2AX phosphorylation after UV irradiation is triggered by DNA repair intermediates and is mediated by the ATR kinase. Carcinogenesis *28*, 2298–2304.

Hanneman, W. H., Legare, M. E., Sweeney, S., and Schimenti, J. C. (1997). Cisplatin increases meiotic crossing-over in mice. Proc. Natl. Acad. Sci. USA *94*, 8681–8685.

Harper, L., Golubovskaya, I., and Cande, W. Z. (2004). A bouquet of chromosomes. J. Cell Sci. *117*, 4025–4032.

Hunter, N. (2008). Hop1 and the meiotic DNA-damage response. Cell *132*, 731–732.

Ismail, I. H., and Hendzel, M. J. (2008). The gamma-H2A.X: is it just a surrogate marker of double-strand breaks or much more? Environ. Mol. Mutagen. *49*, 73–82.

Kaczanowski, A., Gaertig, J., and Kubiak, J. (1985). Effect of the antitubulin drug nocodazole on meiosis and postmeiotic development in *Tetrahymena thermophila*. Induction of achiasmatic meiosis. Exp. Cell Res. *158*, 244–256.

Kanaar, R., and Wyman, C. (2008). DNA repair by the MRN complex: break it to make it. Cell *135*, 14–16.

Keeney, S. (2007). Spo11 and the formation of DNA double-strand breaks in meiosis. In: Recombination and Meiosis, ed. D.-H. Lankenau and R. Egel, Berlin: Springer-Verlag, 81–123.

Knight, Z. A., *et al.* (2006). A pharmacological map of the PI3-K family defines a role for p110α in insulin signaling. Cell *125*, 733–747.

Koszul, R., Kim, K. P., Prentiss, M., Kleckner, N., and Kameoka, S. (2008). Meiotic chromosomes move by linkage to dynamic actin cables with transduction of force through the nuclear envelope. Cell *133*, 1188–1201.

Kurz, E. U., and Lees-Miller, S. P. (2004). DNA damage-induced activation of ATM and ATM-dependent signaling pathways. DNA Repair *3*, 889–900.

Liebe, B., *et al.* (2006). Mutations that affect meiosis in male mice influence the dynamics of the mid-preleptotene and bouquet stages. Exp. Cell Res. *312*, 3768–3781.

Liu, Y., Shreder, K. R., Gai, W., Corral, S., Ferris, D. K., and Rosenblum, J. S. (2005). Wortmannin, a widely used phosphoinositide 3-kinase inhibitor, also potently inhibits mammalian Polo-like kinase. Chem. Biol. *12*, 99–107.

Loidl, J. (1990). The initiation of meiotic chromosome pairing: the cytological view. Genome *33*, 759–778.

Loidl, J., and Scherthan, H. (2004). Organization and pairing of meiotic chromosomes in the ciliate *Tetrahymena thermophila*. J. Cell Sci. *117*, 5791–5801.

Longhese, M. P., Guerini, I., Baldo, V., and Clerici, M. (2008). Surveillance mechanisms monitoring chromosome breaks during mitosis and meiosis. DNA Repair *7*, 545–557.

Lundin, C., North, M., Erixon, K., Walters, K., Jenssen, D., Goldman, A.S.H., and Helleday, T. (2005). Methyl methanesulfonate (MMS) produces heat-

labile DNA damage but no detectable in vivo DNA double-strand breaks. Nucleic Acids Res. *33*, 3799–3811.

Mahadevaiah, S. K., Turner, J.M.A., Baudat, F., Rogakou, E. P., De Boer, P., Blanco-Rodríguez, J., Jasin, M., Keeney, S., Bonner, W. M., and Burgoyne, P. S. (2001). Recombinational DNA double-strand breaks in mice precede synapsis. Nat. Genet. *27*, 271–276.

Marti, T. M., Hefner, E., Feeney, L., Natale, V., and Cleaver, J. E. (2006). H2AX phosphorylation within the G_1 phase after UV irradiation depends on nucleotide excision repair and not DNA double-strand breaks. Proc. Natl. Acad. Sci. USA *103*, 9891–9896.

Mochizuki, K., Novatchkova, M., and Loidl, J. (2008). DNA double-strand breaks, but not crossovers, are required for the reorganization of meiotic nuclei in *Tetrahymena*. J. Cell Sci. *121*, 2148–2158.

Moens, P. B., Bernelot-Moens, C., and Spyropoulos, B. (1989). Chromosome core attachment to the meiotic nuclear envelope regulates synapsis in *Chloealtis* (Orthoptera). Genome *32*, 601–610.

Morrison, T. L., Yakisich, J. S., Cassidy-Hanley, D., and Kapler, G. M. (2005). TIF1 represses rDNA replication initiation, but promotes normal S phase progression and chromosome transmission in *Tetrahymena*. Mol. Biol. Cell *16*, 2624–2635.

Orias, E., Hamilton, E. P., and Orias, J. D. (2000). *Tetrahymena* as a laboratory organism: useful strains, cell culture, and cell line maintenance. In: *Tetrahymena thermophila*, ed. D. J. Asai and J. D. Forney, San Diego: Academic Press, 189–211.

Pandita, T. K., Westphal, C. H., Anger, M., Sawant, S. G., Geard, C. R., Pandita, R. K., and Scherthan, H. (1999). *Atm* inactivation results in aberrant telomere clustering during meiotic prophase. Mol. Cell. Biol. *19*, 5096–5105.

Penkner, A., Portik-Dobos, Z., Tang, L., Schnabel, R., Novatchkova, M., Jantsch, V., and Loidl, J. (2007). A conserved function for a *C. elegans* Com1/Sae2/CtIP protein homologue in meiotic recombination. EMBO J. *26*, 5071–5082.

Peoples-Holst, T. L., and Burgess, S. M. (2005). Multiple branches of the meiotic recombination pathway contribute independently to homolog pairing and stable juxtaposition during meiosis in budding yeast. Genes Dev. *19*, 863–874.

Ray, C., Jr. (1956). Meiosis and nuclear behaviour in *Tetrahymena pyriformis*. J. Protozool. *3*, 88–96.

Richardson, C., Horikoshi, N., and Pandita, T. K. (2004). The role of the DNA double-strand break response network in meiosis. DNA Repair *3*, 1149–1164.

Sanchez-Moran, E., Santos, J. L., Jones, G. H., and Franklin, F.C.H. (2007). ASY1 mediates AtDMC1-dependent interhomolog recombination during meiosis in *Arabidopsis*. Genes Dev. *21*, 2220–2233.

Sarkaria, J. N., Tibbetts, R. S., Busby, E. C., Kennedy, A. P., Hill, D. E., and Abraham, R. T. (1998). Inhibition of phosphoinositide 3-kinase related kinases by the radiosensitizing agent wortmannin. Cancer Res. *58*, 4375–4382.

Sarkaria, J. N., Tibbetts, R. S., Busby, E. C., Kennedy, A. P., Hill, D. E., and Abraham, R. T. (2008). Inhibition of phosphoinositide 3-kinase related kinases by the radiosensitizing agent wortmannin. Cancer Res. *58*, 4375–4382.

Scherthan, H. (2001). A bouquet makes ends meet. Nat. Rev. Mol. Cell. Biol. *2*, 621–627.

Scherthan, H. (2006). Factors directing telomere dynamics in synaptic meiosis. Biochem. Soc. Trans. *34*, 550–553.

Scherthan, H., Weich, S., Schwegler, H., Härle, M., Heyting, C., and Cremer, T. (1996). Centromere and telomere movements during early meiotic prophase of mouse and man are associated with the onset of chromosome pairing. J. Cell Biol. *134*, 1109–1125.

Smart, D. J., Halicka, H. D., Schmuck, G., Traganos, F., Darzynkiewicz, Z., and Williams, G. M. (2008). Assessment of DNA double-strand breaks and gamma H2AX induced by the topoisomerase II poisons etoposide and mitoxantrone. Mutat. Res. Fundam. Mol. Mech. Mutat. *641*, 43–47.

Smith, J. J., Yakisich, J. S., Kapler, G. M., Cole, E. S., and Romero, D. P. (2004). A beta-tubulin mutation selectively uncouples nuclear division and cytokinesis in *Tetrahymena thermophila*. Eukaryot. Cell *3*, 1217–1226.

Song, X. Y., Gjoneska, E., Ren, Q. H., Taverna, S. D., Allis, C. D., and Gorovsky, M. A. (2007). Phosphorylation of the SQ H2A. X motif is required for proper meiosis and mitosis in *Tetrahymena thermophila*. Mol. Cell. Biol. *27*, 2648–2660.

Storlazzi, A., Tessé, S., Gargano, S., James, F., Kleckner, N., and Zickler, D. (2003). Meiotic double-strand breaks at the interface of chromosome movement, chromosome remodeling, and reductional division. Genes Dev. *17*, 2675–2687.

Sugai, T., and Hiwatashi, K. (1974). Cytologic and autoradiographic studies of the micronucleus at meiotic prophase in *Tetrahymena pyriformis*. J. Protozool. *21*, 542–548.

Tomita, K., and Cooper, J. P. (2007). The telomere bouquet controls the meiotic spindle. Cell *130*, 113–126.

Trelles-Sticken, E., Loidl, J., and Scherthan, H. (1999). Bouquet formation in budding yeast: initiation of recombination is not required for meiotic telomere clustering. J. Cell Sci. *112*, 651–658.

Wolfe, J., Hunter, B., and Adair, W. S. (1976). A cytological study of micronuclear elongation during conjugation in *Tetrahymena*. Chromosoma *55*, 289–308.

Yakisich, J. S., and Kapler, G. M. (2004). The effect of phosphoinositide 3-kinase inhibitors on programmed nuclear degradation in *Tetrahymena* and fate of surviving nuclei. Cell Death Diff. *11*, 1146–1149.

Yakisich, J. S., Sandoval, P. Y., Morrison, T. L., and Kapler, G. M. (2006). TIF1 activates the intra-S-phase checkpoint response in the diploid micronucleus and amitotic polyploid macronucleus of *Tetrahymena*. Mol. Biol. Cell *17*, 5185–5197.

Yamamoto, A., and Hiraoka, Y. (2001). How do meiotic chromosomes meet their homologous partners?: lessons from fission yeast. Bioessays *23*, 526–533.

Zickler, D. (2006). From early homologue recognition to synaptonemal complex formation. Chromosoma *115*, 158–174.

Zickler, D., and Kleckner, N. (1998). The leptotene-zygotene transition of meiosis. Annu. Rev. Genet. *32*, 619–697.